



## ***In Silico* Exploration of the Safety Profile of Bioactive Compounds Extracted from Prickly Pear Cladodes (*Opuntia ficus-indica*): Toward Therapeutic Applications**

[Benghanem Soumia\\*](#) , [Chenafa Hadjer](#) , [Berrabah Ammaria](#)   
[Benahmed Isam](#) , [Aouad Ismail](#) 

Department of pharmacy , Faculty of Medecine, University Aboubaker Belkaid  
13000, Tlemcen, ALgeria

\*Corresponding author : [soumia.benghanem@univ-tlemcen.dz](mailto:soumia.benghanem@univ-tlemcen.dz)

Received: 12/12/2024

Accepted: 02/03/2025

<https://doi.org/10.38093/cupmap.1600535>

### Abstract

*Opuntia ficus-indica*, commonly known as prickly pear, is a medicinal plant rich in bioactive compounds such as flavonoids and alkaloids, which have gained increasing interest for their therapeutic potential. This study employs in silico approaches to evaluate the physicochemical properties, bioavailability, and toxicity of ten compounds found in prickly pear cladodes. Molecular modeling tools, including SwissADME, ProTox-II, and Molinspiration, were used to predict their pharmacokinetic and pharmacological profiles. The results indicate that most compounds exhibit favorable aqueous solubility and permeability, supporting good digestive absorption. However, glycosylated flavonoids, such as isoquercitrin and rutin, showed limited membrane permeability but may undergo metabolic transformation into more bioavailable forms, such as quercetin and kaempferol. Toxicity assessments classified most compounds as low risk, though isoquercitrin exhibited a potential genotoxic signal in the Ames test, warranting further investigation. Additionally, molecular docking analysis identified quercetin as a promising inhibitor of GSK-3 $\beta$ , a key enzyme involved in metabolic, inflammatory, neurodegenerative, and oncological diseases. Notably, quercetin demonstrated a stronger binding affinity for GSK-3 $\beta$  than the reference inhibitor IXM, reinforcing its potential for drug development. Overall, these findings highlight the relevance of in silico analyses in early-stage drug discovery and provide a strong basis for further in vitro and in vivo studies to validate the therapeutic potential of these bioactive compounds.

**Key Words:** *Opuntia ficus-indica*, Cladodes, Safety ,Bioactivity,Quercetin, GSK-3 $\beta$ , In Silico.

© CUPMAP. All rights reserved.

### Introduction

*Opuntia ficus-indica*, commonly known as the prickly pear cactus, belongs to the Cactaceae family and has been widely used in traditional medicine to treat various ailments, including diabetes, hypertension, cardiovascular diseases, and inflammation.

Its medicinal use dates back several centuries, particularly in Latin America and certain regions of the Middle East, where its antidiabetic, anti-inflammatory, and antioxidant properties have been extensively exploited (Del Socorro Santos Díaz, 2017; Wang, 2023). The cladodes of this plant are particularly valued for their richness in

bioactive compounds, whose consumption has been associated with numerous health benefits (Guevara-Figueroa et al., 2010; Martins et al., 2023). Although *Opuntia ficus-indica* is increasingly used for its medicinal properties, the bioactive mechanisms underlying its therapeutic effects remain poorly understood.

This study aims to explore, using in silico approaches, the physicochemical, pharmacological, and toxicological properties of ten bioactive flavonoids extracted from the cladodes of *Opuntia ficus-indica*. We seek to assess their safety as well as their pharmacological potential. In particular, we focus on the inhibition of glycogen synthase kinase-3 $\beta$  (GSK-3 $\beta$ ), an enzyme involved in several chronic diseases, including diabetes and cancer (Beurel et al., 2015). We evaluate the efficacy of quercetin, a key metabolite of isoquercitrin, known for its multiple biological activities, as a potential inhibitor of GSK-3 $\beta$  (Valentová et al., 2014).

To achieve this, we use the molecular docking technique, a well-established method for identifying GSK-3 $\beta$  inhibitors, whether natural or synthetic (Benghanem et al., 2023; Benlazar et al., 2024). This work aims to provide a solid scientific basis for the safe and therapeutic exploitation of compounds extracted from the prickly pear cactus (Kashif et al., 2022).

## 2. Material and Methods

**2.1. Molecular Structure Collection and Preparation:** The chemical structures of ten bioactive compounds extracted from *Opuntia ficus-indica* cladodes were retrieved from the PubChem database (<http://pubchem.ncbi.nlm.nih.gov/>) using their respective CID identifiers. (Guevara-Figueroa et al., 2010). Each structure was downloaded in canonical SMILES format to ensure uniform molecular modeling input. The structures were

optimized using ChemDraw Professional 22.0 to correct molecular geometry errors and generate high-quality 2D representations. These optimized structures were used as input for in silico prediction platforms, as detailed in Table 1.

### 2.2. Evaluation of Physicochemical Properties

Each compound underwent QSAR-based prediction analysis, with results expressed as qualitative indicators using a color-coding system for easier interpretation:

- **Red:** High risk of adverse effects
- **Yellow:** Tolerable result
- **Green:** Desired behavior (Kumar et al., 2017)

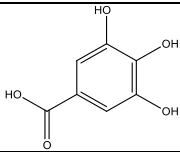
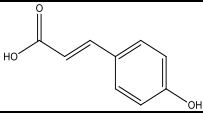
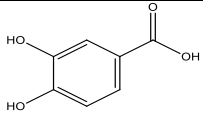
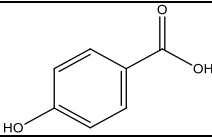
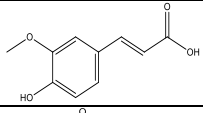
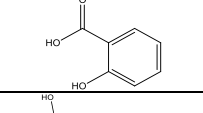
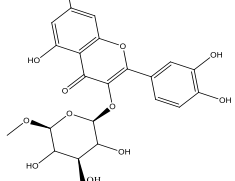
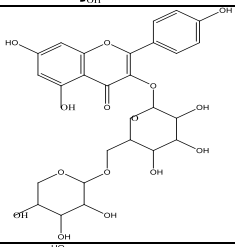
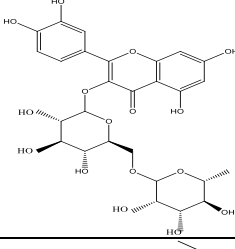
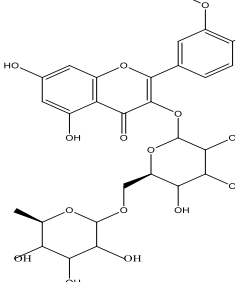
The evaluation followed Lipinski's "Rule of Five," complemented by additional criteria such as aqueous solubility and topological polar surface area (TPSA) (Lipinski et al., 1997).

**2.2.1. Molecular Weight (MW):** The molecular weight of each compound was calculated using the SwissADME server (<http://www.swissadme.ch/>). A molecular weight below 500 Da was considered acceptable based on Lipinski's rule (Lipinski et al., 1997). Results are listed in Table 2.

**2.2.2. Hydrogen Bond Donors and Acceptors:** The number of hydrogen bond donors and acceptors was determined using SwissADME. A maximum of five hydrogen bond donors and ten acceptors was set according to Lipinski's rule (Lipinski et al., 1997). The results are clearly presented in Table 2.

**2.2.3. Aqueous Solubility (LogS):** Aqueous solubility was determined using OSIRIS (<https://www.organic-chemistry.org/prog/peo/logS.html>). Values higher than -4 indicated good solubility. Results are presented in Table 2.

**Table 1.** CID Identifiers, SMILES, and Structures of the Tested Molecules

Ligands	Molécules	CID PubChem	PW	Structures	SMILES
L1	Acide gallique	24721416	188.13		<chem>C1=C(C=C(C(=C1O)O)O)C(=O)O</chem>
L2	Acide coumarique	1549106	164.16		<chem>C1=CC(=CC=C1C=CC(=O)O)O</chem>
L3	Acide 3,4-dihydroxybenzoïque	72	154.12		<chem>C1=CC(=C(C=C1C(=O)O)O)O</chem>
L4	acide 4-hydroxybenzoïque	135	138.12		<chem>C1=CC(=CC=C1C(=O)O)O</chem>
L5	Acide férulique	445858	194.18		<chem>COC1=C(C=CC(=C1)C=CC(=O)O)O</chem>
L6	Acide salicylique	338	138.12		<chem>C1=CC=C(C(=C1)C(=O)O)O</chem>
L7	Isoquercitrine	5280804	464.4		<chem>C1=CC(=C(C=C1C2=C(C(=O)C3=C(C=C(C=C3O2)O)O)OC4C(C(C(C(O4)CO)O)O)O)O)O</chem>
L8	Nicotiflorine	5318767	594.5		<chem>C[C@@H]1O[C@@H](OC[C@@H]2O[C@@H](OC3=C(OC4=C(C(O)=CC(O)=C4)C3=O)C3=CC=C(O)C=C3)[C@H](O)[C@@H](O)[C@@H]2O)[C@@H](O)[C@@H](O)[C@@H]1O</chem>
L9	Rutine	5280805	610.5		<chem>C[C@@H]1O[C@@H](OC[C@@H]2O[C@@H](OC3=C(OC4=C(C(O)=CC(O)=C4)C3=O)C3=CC=C(O)C(O)=C3)[C@H](O)[C@@H](O)[C@@H]2O)[C@@H](O)[C@@H](O)[C@@H]1O</chem>
L10	Narcissine	5481663	624.5		<chem>C1CN2CC3=CC4=C(C=C3C5C2C1=CC(C5O)OC)O4</chem>

**2.2.4. Topological Polar Surface Area (TPSA):** TPSA was calculated using OSIRIS (<https://www.organic-chemistry.org/prog/peo/>). A  $TPSA \leq 140 \text{ \AA}^2$  was associated with good membrane permeability (Veber *et al.*, 2002). Results are shown in Table 2.

**2.2.5. Octanol-Water Partition Coefficient (LogP):** LogP was calculated using SwissADME (<http://www.swissadme.ch/>). A value between 0 and 5 indicated a good hydrophilic-lipophilic balance, essential for membrane permeability (Kaiser *et al.*, 1982). Results are detailed in Table 2.

**Table 2.** Lipinski's Rule of Five from SwissADME, TPSA, and log S from OSIRIS

				Lipinski's Rule of Five				
				Molecular Weight (g/mol)	Lipophilicity (MLogP)	Hydrogen Bond Donors	Hydrogen Bond Acceptors	No. of Rule Violations
N°	CID	Solubility log $\Sigma$	TPSA $\text{\AA}^2$	Lessthan 500 Dalton	Lessthan 5	Lessthan 5	Lessthan 10	Lessthan 2 Violations
L1	370	-1.07	107.22	170.12	1.28	2	3	0 violation
L2	1549106	-1.7	57.53	164.16	1.28	2	3	0 violation
L3	72	-1.04	77.76	154.12	0.40	3	4	0 violation
L4	135	-1.33	57.53	138.12	0.99	2	4	0 violation
L5	445858	-1.72	66.76	194.18	1.00	3	4	0 violation
L6	338	-1.33	57.53	138.12	0.99	2	3	0 violation
L7	5280804	-2.19	206.60	464.38	-2.59	8	12	2 violations
L8	5318767	-2.69	245.29	594.52	-3.43	9	15	3, violations
L9	5280805	-2.40	265.52	610.52	-3.89	10	16	3, violations
L10	72378	-2.78	62.16	287.31	1.08	2	5	0 violation

## 2.3. Prediction of Toxicity

### 2.3.1. Acute Toxicity Prediction (LD50):

Acute toxicity was predicted using Protox II ([https://tox-new.charite.de/protox\\_II/](https://tox-new.charite.de/protox_II/)). The median lethal doses (LD50) were expressed in mg/kg. The results are presented in Table 3.

**2.3.2. Specific Toxicity:** The evaluation of risks related to mutagenicity, hepatotoxicity, and irritation was performed using AdmetSAR (<https://lmmd.ecust.edu.cn/>),

[admet.sar2/](https://admet.sar2/)), OSIRIS, and Protox. The results are provided in Tables 4 and 5.

### 2.4. Prediction of Biological Activity

Biological activity predictions focused on G protein-coupled receptors (GPCRs), ion channels, kinases, and nuclear receptors, which are crucial in the development of new drugs. The Molinspiration tool (<https://www.molinspiration.com/>) was used to evaluate the bioactivity scores for the targets. These scores are presented in Table 6.

**Table 3.** Toxicity Classification of Tested Compounds Based on LD<sub>50</sub> Values Predicted by Protox-II

Ligands Classes	L1	L2	L3	L4	L5	L6	L7	L8	L9	L10
Predicted Toxicity Class	4	5	4	5	4	4	5	5	5	3
Classe I : extrêmement toxique (LD50 ≤ 5)	-	-	-	-	-	-	-	-	-	-
Classe II : très toxique (5 < LD50 ≤ 50)	-	-	-	-	-	-	-	-	-	-
Classe III : modérément toxique (50 < LD50 ≤ 300)	-	-	-	-	-	-	-	-	-	+
Classe IV : légèrement toxique (300 < LD50 ≤ 2000)	+	-	+	-	+	+	-	-	-	-
Classe V : non toxique (2000 < LD50 ≤ 5000)	-	+	-	+	-	-	+	+	+	-
Classe VI : sequirise (LD50 > 5000)	-	-	-	-	-	-	-	-	-	-

**Table 4.** Predicted Toxicity Risks According to OSIRIS and AdmetSAR

serveur	OSIRIS	ADMETSAR	
Ligands	Irritant	Ames toxicity	Carcinogenicity
L1		Non toxic	Non carcinogenic
L2		Non toxic	Non carcinogenic
L3		Non toxic	Non carcinogenic
L4		Non toxic	Non carcinogenic
L5		Non toxic	Non carcinogenic
L6		Non toxic	Non carcinogenic
L7		Toxic	Non carcinogenic
L8		Non toxic	Non carcinogenic
L9		Non toxic	Non carcinogenic
L10		Non toxic	Non carcinogenic

**Table 5.** Report on Organ Toxicity, General Toxicity, and Stress Response Pathways by Protox (A: Presence of Toxicity , I: Absence of Toxicity)

Ligands		L1	L2	L3	L4	L5	L6	L7	L8	L9	L10	
Classification	Target											
	Organ toxicity	Hepatotoxicity	0.61 I	I 0.51	I 0.59	I 0.52	I 0.51	A 0.51	I 0.82	0.80 I	0.88 I	0.87 I
		Mutagenicity	0.94 I	I 0.93	I 0.97	I 0.99	I 0.96	I 0.98	I 0.76	0.88 I	0.88 I	0.95 I
	Stress response	Nuclear factor (erythroid-derived 2)-like 2/antioxidant	0.85 I	I 0.94	I 0.98	I 1.0	I 0.90	I 0.99	I 0.98	0.99 I	0.99 I	0.92 I

Nuclear receptor signalling pathways	responsive element (nrf2/ARE)										
	Heat shock factor response element (HSE)	0.85 I	I 0.94	I 0.98	I 1.0	I 0.90	I 0.99	I 0.98	<b>0.99</b> I	0.99 I	0.92 I
	Mitochondrial Membrane Potential (MMP)	0.97 I	I 0.97	I 0.99	I 0.99	I 0.92	I 0.99	I 0.98	<b>0.97</b> I	0.97 I	0.79 I
	Phosphoprotein (Tumor Suppressor) p53	0.97 I	I 0.95	I 0.99	I 0.99	I 0.92	I 0.99	A 0.5	<b>0.90</b> I	0.90 I	0.90 I
	ATPase family AAA domain-containing protein 5 (ATAD5)	0.99 I	I 0.96	I 1.0	I 0.99	I 0.93	I 0.99	I 1.0	<b>0.99</b> I	0.99 I	0.78 I
	Aryl hydrocarbon Receptor (AhR)	0.90 I	I 0.96	I 0.96	I 0.96	I 0.94	I 0.98	I 0.92	<b>0.83</b> I	0.83 I	0.71 I
	Androgen Receptor (AR)	0.97 I	I 0.87	I 0.84	I 0.99	I 0.83	I 0.99	I 0.90	<b>0.98</b> I	0.98 I	0.96 I
	Androgen Receptor Ligand Binding Domain (AR-LBD)	1.0 I	I 0.99	I 1.0	I 1.0	I 0.99	I 1.0	I 0.98	<b>0.99</b> I	0.99 I	0.97 I
	Aromatase	<b>0.99</b> I	I 0.99	I 0.99	I 0.99	I 0.99	I 1.0	I 1.0	<b>0.99</b> I	0.99 I	0.92 I
	Estrogen Receptor Alpha (ER)	<b>0.89</b> I	I 0.97	I 0.99	I 0.99	I 0.96	I 0.96	I 0.91	<b>0.95</b> I	0.95 I	0.80 I
	Estrogen Receptor Ligand Binding Domain (ER-LBD)	<b>0.9</b> I	I 0.97	I 0.95	I 0.98	I 0.96	I 0.98	I 0.99	<b>0.99</b> I	0.99 I	0.95 I

**Table 6.** Predicted Bioactivity Scores for Drug Targets Including GPCR Ligands, Kinase Inhibitors, Ion Channel Modulators, and Nuclear Receptor Ligands (by Molinspiration)

Molinspiration bioactivity	GPCR ligand	Ion channel modulator	Kinase inhibitor	Nuclear receptor ligand	Enzyme inhibitor	Protease inhibitor
L1	-0.77	-0.26	-0.88	-0.52	-0.17	-0.94
L2	-0.56	-0.26	-0.91	-0.12	-0.15	-0.87
L3	-0.88	-0.35	-1.10	-0.58	-0.34	-1.09
L4	-0.98	-0.39	-1.21	-0.62	-0.41	-1.19
L5	-0.47	-0.30	-0.72	-0.14	-0.12	-0.81
L6	-0.98	-0.43	-1.22	-0.79	-0.41	-1.14
L7	0.06	-0.04	0.13	0.20	0.42	-0.06
L8	-0.01	-0.43	-0.09	-0.17	0.18	-0.04
L9	-0.05	-0.52	-0.14	-0.23	0.12	-0.07
L10	0.43	0.25	-0.25	0.10	0.66	0.07

## 2.5. Molecular Docking Study and Binding Mode

**2.5.1. Protein Preparation:** The crystal structure of GSK-3 $\beta$  (PDB ID: 1Q5K, Resolution: 1.94 Å) was downloaded from the Protein Data Bank (<https://www.rcsb.org/>). Chain B was removed, and water molecules were eliminated. The structure was minimized using the OPLS force field.

**2.5.2. Ligand Preparation:** The deglycosylated metabolite of isoquercitrin, quercetin, was prepared using LigPrep (v4.7,

Schrödinger 2019-3). The generated structures were used for docking simulations.

**2.5.3. Cross-Docking:** A docking test was performed with the reference inhibitor IXM (indurbin), a known GSK-3 $\beta$  ligand. The docking score of quercetin was compared to that of IXM. The results are presented in Table 7, with a detailed analysis of the binding mode of quercetin in the ATP-binding site of the receptor.

**Table 7:** Docking Scores of Quercetin

Composés	Code CID	Nombre de poses	Glide score	State penalty	Docking score	E model
Quercétine	5280343	7	-10,6	0,03	-10,57	-55,46

## 3. Results and Discussion

### 3.1. Evaluation of Physicochemical Properties

**3.1.1. Lipinski's Rule Compliance and Accessible Polar Surface Area (TPSA):** The evaluation of compounds L1 to L6 and L10 shows that they comply with Lipinski's rule, having molecular weights below 500 Da, a limited number of hydrogen bond donors and acceptors, and a TPSA less than 140 Å<sup>2</sup>, suggesting favorable oral absorption potential (Veber *et al.*, 2002; Lipinski *et al.*, 1997). In contrast, compounds L7 (isoquercitrin), L8 (nicotiflorin), and L9 (rutin) do not meet these criteria, as they have high molecular weights and TPSA values well above 140 Å<sup>2</sup>, indicating reduced membrane permeability and limited intestinal absorption. This result is consistent with that of Hiremath for isoquercitrin (Hiremath *et al.*, 2021).

**3.1.2. Solubility (log S):** Adequate solubility is crucial for optimal absorption. Compounds with a log S lower than -4 are considered

poorly soluble, which may limit their bioavailability. However, all compounds exhibit moderate log S values, suggesting sufficient solubility for digestive absorption. This result is consistent with that of Hiremath for isoquercitrin (Hiremath *et al.*, 2021) and that of Souza for rutin (Souza *et al.*, 2023).

**3.1.3. Lipophilicity (MLogP):** Compounds L1 to L6, and L10, and present MLogP values ranging from -0.4 to 5, indicating optimal intestinal absorption. In contrast, compounds L7, L8, and L9 exhibit negative MLogP values (<-2), reflecting excessive hydrophilicity and reduced ability to cross biological membranes.

**3.1.4. Reevaluation of Metabolites:** Despite initially unfavorable physicochemical properties for optimal absorption, the glycosylated flavonoid derivatives (L7, L8, L9) undergo deglycosylation in the gastrointestinal tract, producing metabolites with improved physicochemical characteristics. For instance, L7 (isoquercitrin) is transformed into quercetin, with a molecular weight of 302.24 g/mol and

a TPSA of 131.36 Å<sup>2</sup>. L8 (nicotiflorine) is metabolized to kaempferol, with a molecular weight of 286.24 g/mol and a TPSA of 107.22 Å<sup>2</sup>, while L9 (rutin) also produces quercetin. These metabolites show molecular weights and TPSA values compatible with good oral absorption. In terms of lipophilicity, quercetin and kaempferol have moderate MLogP values (1.73 and 1.38, respectively), indicating an enhanced ability to traverse lipid membranes and be efficiently absorbed.

### 3.2. Toxicity Evaluation

**3.2.1. Acute Toxicity (LD50):** The compounds were classified into five toxicity categories based on the OECD classification system:

- Class I: Extremely toxic (LD50 < 5 mg/kg)
- Class II: Very toxic (5–50 mg/kg)
- Class III: Moderately toxic (50–300 mg/kg)
- Class IV: Slightly toxic (300–2000 mg/kg)
- Class V: Non-toxic (LD50 > 2000 mg/kg)

Compounds with an LD50 greater than 2000 mg/kg were considered safe for potential use. All of the tested compounds fall into Classes III and above. Detailed results are presented in Table 03.

#### 3.2.2. Specific Toxicity

**3.2.2.1. Irritability:** L1 (gallagic acid) and L6 (salicylic acid) were identified as irritants (marked in orange in Table 4), indicating that they could cause skin or mucous membrane irritation. On the other hand, the other ligands (L2 to L5, L7 to L10) showed no irritant properties, which is favorable for potential oral or topical applications.

**3.2.2.2. Genotoxicity: Ames Test and Mutagenicity:** L7 (isoquercitrin) was classified as toxic in the Ames test, which could indicate a genotoxic potential. However, other studies have shown that isoquercitrin in an inclusion complex (IQC-γCD) does not exhibit genotoxicity in experimental models (Kapoor *et al.*, 2022).

The other compounds were considered non-mutagenic according to ProTox-II, indicating a reassuring safety profile for long-term use. Results are shown in Tables 4 and 5. The Ames toxicity and hepatotoxicity results are consistent with those of Souza for isoquercitrin and rutin (Souza *et al.*, 2023).

**3.2.2.3. Carcinogenicity:** All compounds were classified as non-carcinogenic, which further supports their safety profile for consumption or further development. This is detailed in Table 4.

**3.2.2.4. Hepatotoxicity:** L6 (salicylic acid) may present a risk of hepatotoxicity. In contrast, other ligands seem to be better tolerated by the liver, as indicated in Table 5.

**3.2.2.5. Stress Response Pathways and Nuclear Receptor Signaling Pathways:** Interference was observed for L7 concerning the phosphoprotein p53 (tumor suppressor). No other interference with stress response pathways or nuclear receptor signaling pathways was recorded, as shown in Table 5.

### 3.3. Prediction of Biological Activity

The prediction of biological activity for several compounds extracted from prickly pear cladodes revealed promising therapeutic potential. Molecules such as L7 (isoquercitrin), L10 (narcissine) were predicted to target multiple biological activities. Specifically:

**L7 (isoquercitrin)** is predicted to interact with G-protein-coupled receptors (GPCRs), act as a kinase inhibitor, bind to nuclear receptors, and inhibit enzymes.

**L10 (narcissine)** is predicted to modulate ion channels, inhibit proteases, and interact with nuclear receptors. Among these, **isoquercitrin (L7)** stands out for its predicted kinase inhibitory activity, which led to its selection for further investigation, specifically targeting GSK-3β.

### 3.4. Molecular Docking Study

**3.4.1. Scoring Analysis:** Molecular docking results, presented in Table 7, show that the best pose was selected based on the docking score, with lower scores indicating higher affinity of the molecule for the receptor. Quercetin achieved a docking score of **-10.57 kcal/mol**, which is lower (indicating higher

affinity) than the reference inhibitor **IXM** with a score of **-9.313 kcal/mol**.

**3.4.2. Binding Mode:** The molecular interactions between quercetin and the reference inhibitor IXM with residues from the active site of GSK-3 $\beta$  (PDB ID: 1Q1K) were analyzed. The 2D interaction diagrams for IXM and quercetin are shown in Figures 1 and 2, respectively.

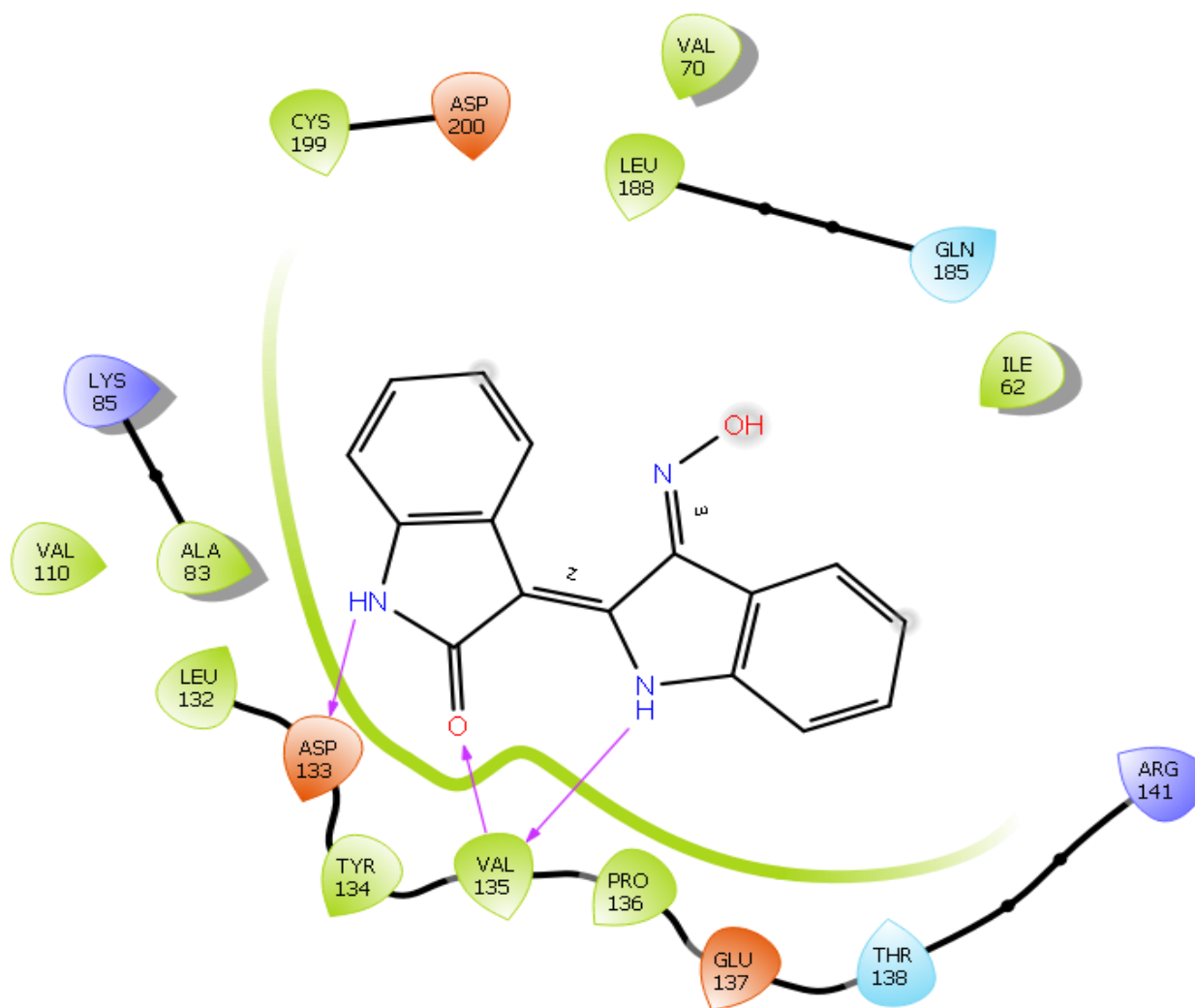


**Figure 1.** 2D Interactions of IXM (Indirubin) with GSK-3 $\beta$  after Cross-Docking in PDB ID: 1Q5K

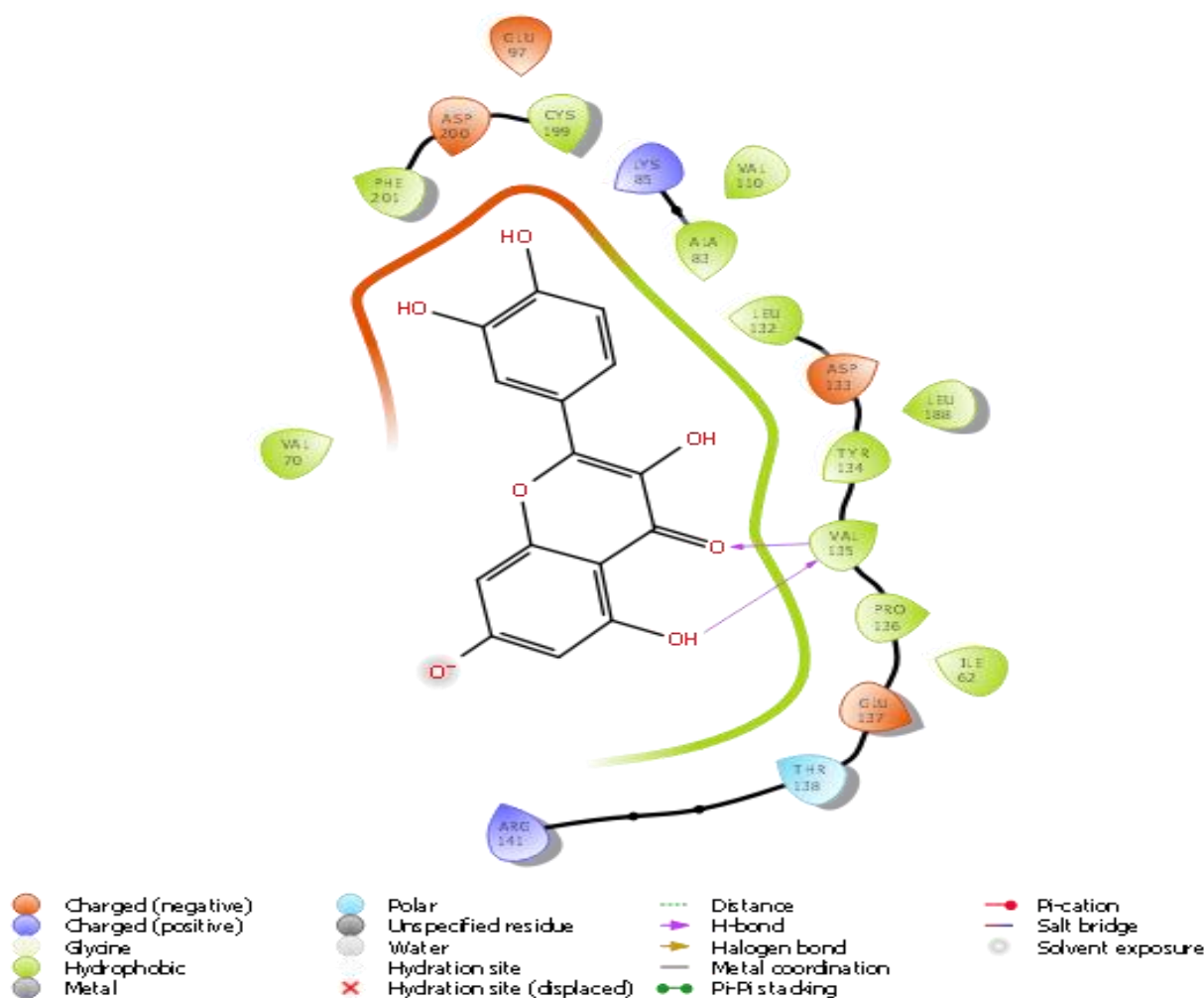


**Figure 2.** 2D Interactions of Quercetin with GSK-3 $\beta$  after Docking in PDB ID: 1Q5K

Both quercetin and IXM show strong inhibition, mainly due to hydrogen bonding with the **Val135** residue. Notably, while IXM forms an additional hydrogen bond with **Asp133**, quercetin displays a lower binding energy score, indicating a stronger affinity for the active site. This binding mode aligns with the known mechanism of GSK-3 $\beta$  inhibition, where hydrogen bonds with **Val135** and **Asp133** are crucial for effective inhibition, as outlined by Arfeen et al. (Arfeen et al., 2016). This result for quercetin is consistent with the findings of Baby et al on quercetin and isoquercitrin, describing their action as inhibitors of serine/threonine kinase, which belongs to the GSK3 $\beta$  superfamily (Baby et al., 2016).

The findings of this study align with previous research on *Opuntia ficus-indica* and its bioactive compounds. Consistent with our results, Hiremath et al. (2021) reported that isoquercitrin exhibits limited membrane permeability. Similarly, Souza et al. (2023) highlighted the low solubility and moderate absorption potential of rutin, further supporting our observations on its pharmacokinetic profile.

In our study, we found that its deglycosylated metabolites, quercetin and kaempferol, formed during metabolism in the small intestine, displayed significantly improved bioavailability. Moreover, molecular docking analysis identified quercetin as a potent GSK-3 $\beta$  inhibitor, exhibiting a higher binding

affinity than the reference inhibitor IXM. This is particularly relevant given the involvement of GSK-3 $\beta$  in various diseases, including diabetes, neurodegenerative disorders (e.g., Alzheimer's and Parkinson's), and inflammatory conditions. Our findings align with those of Baby et al. (2016), who previously identified flavonoids as promising regulators of GSK-3 $\beta$ . These results reinforce the potential of *Opuntia ficus-indica* cladodes as valuable sources of bioactive molecules for drug development.

Despite these promising insights, our study has certain limitations. While in silico predictions are valuable for early-stage screening, they require experimental validation through in vitro and in vivo studies. Computational models alone cannot fully assess crucial factors such as metabolic stability, enzymatic transformations, and long-term toxicity. Future research should focus on pharmacokinetic studies and preclinical trials to confirm the bioavailability and therapeutic potential of these cladode-derived compounds.

Overall, this study provides key insights into the pharmacokinetic properties, safety profile, and therapeutic potential of bioactive compounds contained in *Opuntia ficus-indica* cladodes, paving the way for further experimental validation and potential pharmaceutical applications.

#### 4. Conclusion

This study evaluated the physicochemical properties, toxicity, and biological activity of major compounds extracted from prickly pear cladodes. Most compounds exhibited favorable physicochemical properties supporting good oral absorption. However, glycosylated flavonoids (L7, L8, L9) showed reduced permeability, though their deglycosylated metabolites, such as quercetin and kaempferol, demonstrated improved bioavailability. Regarding toxicity, most compounds were classified as low risk,

yet isoquercitrin exhibited a potential genotoxic signal in the Ames test, consistent with previous findings, highlighting the need for further investigation. Molecular docking analysis revealed that quercetin displayed a stronger binding affinity for GSK-3 $\beta$  than the reference inhibitor IXM, reinforcing its potential role in targeting this enzyme. Given the involvement of GSK-3 $\beta$  in various pathologies, including diabetes, inflammation, cancer, and neurodegenerative diseases, these findings suggest that quercetin and related metabolites could serve as promising therapeutic candidates.

Overall, this study underscores the importance of in silico assessments in early drug discovery and provides a strong rationale for conducting further in vitro and in vivo studies to validate the therapeutic potential of these bioactive compounds.

#### Acknowledgements

-

#### Author Contribution

All authors declare equal contribution to the design and experimental work, interpretation of the results and editing the manuscript.

#### Conflicts of Interest

The authors declared no conflict of interest.

#### References

1. Del Socorro Santos Díaz, M., Barba de la Rosa, A. P., Héliès-Toussaint, C., Guéraud, F., & Nègre-Salvayre, A. (2017). *Opuntia spp.*: Characterization and Benefits in Chronic Diseases. *Oxidative Medicine and Cellular Longevity*, 2017, 8634249. <https://doi.org/10.1155/2017/8634249>
2. Wang, J., Rani, N., Jakhar, S., Redhu, R., Kumar, S., Kumar, S., Kumar, S., Devi, B., Simal-Gandara, J., Shen, B., & Singla, R. K. (2023). *Opuntia ficus-indica* (L.) Mill. - anticancer properties and phytochemicals: current trends and future perspectives. *Frontiers in Plant Science*, 14, 1236123. <https://doi.org/10.3389/fpls.2023.1236123>

3. Guevara-Figueroa, T., Jiménez-Islas, H., et al. (2010). Proximate composition, phenolic acids, and flavonoids characterization of commercial and wild nopal (*Opuntia spp.*). *Journal of Food Composition and Analysis*, 23(6), 525-532.
4. Martins, M., Ribeiro, M. H., & Almeida, C. M. M. (2023). Physicochemical, Nutritional, and Medicinal Properties of *Opuntia ficus-indica* (L.) Mill. and Its Main Agro-Industrial Use: A Review. *Plants*, 12(7), 1512. <https://doi.org/10.3390/plants12071512>
5. Beurel, E., Grieco, S. F., & Jope, R. S. (2015). Glycogen synthase kinase-3 (GSK3): regulation, actions, and diseases. *Pharmacology & Therapeutics*, 148, 114-131. <https://doi.org/10.1016/j.pharmthera.2014.11.016>
6. Valentová, K., Vrba, J., Bancířová, M., Ulrichová, J., & Křen, V. (2014). Isoquercitrin: Pharmacology, toxicology, and metabolism. *Food and Chemical Toxicology*, 68, 267-282. <https://doi.org/10.1016/j.fct.2014.03.018>
7. Benghanem, S., Mesli, F., Aoul, H. F. Z., Nacereddine, C., Hadjer, C., & Abdellatif, M. (2023). Discovery of novel and highly potential inhibitors of glycogen synthase kinase 3-beta (GSK-3 $\beta$ ) through structure-based pharmacophore modeling, virtual computational screening, docking and in silico ADMET analysis. *Journal of Biomolecular Structure and Dynamics*. <https://doi.org/10.1080/07391102.2023.2238062>
8. Benlazar, M. I., & Merzoug, S. (2024). In-vitro antioxidant and in-silico wound healing activity of *Quercus infectoria* dry extract. *Current Perspectives on Medicinal and Aromatic Plants*, 7(1),41-47. <https://doi.org/10.38093/cupmap.1488652>
9. Kashif, R. R., D'Cunha, N. M., Mellor, D. D., Alexopoulos, N. I., Sergi, D., & Naumovski, N. (2022). Prickly Pear Cacti (*Opuntia spp.*) Cladodes as a Functional Ingredient for Hyperglycemia Management: A Brief Narrative Review. *Medicina* (Kaunas, Lithuania), 58(2), 300. <https://doi.org/10.3390/medicina58020300>
10. Kumar, T. A., Kabilan, S., et al. (2017). Screening and Toxicity Risk Assessment of Selected Compounds to Target Cancer using QSAR and Pharmacophore Modelling. *International Journal of PharmTech Research*, 10(4), 219-224.
11. Lipinski, C. A., Lombardo, F., Dominy, B. W., & Feeney, P. J. (1997). Experimental and computational approaches to estimate solubility and permeability in drug discovery and development settings. *Advanced Drug Delivery Reviews*, 23(1-3), 3-25.
12. Veber, D. F., Johnson, S. R., et al. (2002). Molecular properties that influence the oral bioavailability of drug candidates. *Journal of Medicinal Chemistry*, 45(12), 2615-2623.
13. Kaiser, K. L., & Valdmanis, I. (1982). Apparent octanol/water partition coefficients of pentachlorophenol as a function of pH. *Canadian Journal of Chemistry*, 60(16), 2104-2106.
14. Hiremath, S., Kumar, H. D. V., Nandan, M., Mantesh, M., Shankarappa, K. S., Venkataravanappa, V., Basha, C. R. J., & Reddy, C. N. L. (2021). In silico docking analysis revealed the potential of phytochemicals present in *Phyllanthus amarus* and *Andrographis paniculata*, used in Ayurveda medicine in inhibiting SARS-CoV-2. *3 Biotech*, 11(2), 44. <https://doi.org/10.1007/s13205-020-02578-7>
15. El-Mostafa, K., El Kharrassi, Y., Badreddine, A., Andreoletti, P., Vamecq, J., El Kebbij, M. S., Latruffe, N., Lizard, G., Nasser, B., & Cherkaoui-Malki, M. (2014). Nopal Cactus (*Opuntia ficus-indica*) as a Source of Bioactive Compounds for Nutrition, Health and Disease. *Molecules*, 19(9), 14879-14901. <https://doi.org/10.3390/molecules190914879>
16. Souza, H. C. A., Souza, M. D. A., Sousa, C. S., Viana, E. K. A., Alves, S. K. S., Marques, A. O., Ribeiro, A. S. N., de Sousa do Vale, V., Islam, M. T., de Miranda, J. A. L., da Costa Mota, M., & Rocha, J. A. (2023). Molecular Docking and ADME-TOX Profiling of *Moringa oleifera* Constituents against SARS-CoV-2. *Advances in Respiratory Medicine*, 91(6), 464-485. <https://doi.org/10.3390/arm91060035>
17. Kapoor, M. P., Moriwaki, M., Timm, D., Satomoto, K., & Minegawa, K. (2022). Genotoxicity and mutagenicity evaluation of isoquercitrin- $\gamma$ -cyclodextrin molecular inclusion complex using Ames test and a combined micronucleus and comet assay in rats. *The Journal of Toxicological Sciences*, 47(6), 221-235. <https://doi.org/10.2131/jts.47.221>
18. Arfeen, M., Bhagat, S., Patel, R., Prasad, S., Roy, I., Chakraborti, A. K., & Bharatam, P. V. (2016). Design, synthesis and biological evaluation of 5-benzylidene-2-iminothiazolidin-4-ones as selective GSK3 $\beta$  inhibitors. *European Journal of Medicinal Chemistry*, 121, 727-736. <https://doi.org/10.1016/j.ejmech.2016.04.075>
19. Baby, B., Antony, P., Al Halabi, W., Al Homedi, Z., & Vijayan, R. (2016). Structural insights into the polypharmacological activity of quercetin on serine/threonine kinases. *Drug design, development and therapy*, 10, 3109-3123. <https://doi.org/10.2147/DDDT.S118423>